京都大学防災研究所年報 第 61 号 B 平成 30 年
DPRI Annuals, No. 61 B, 2018

Evaluation of Deep S-wave Velocity Profiles in Sagaing City, Myanmar from Long-Period Microtremor Array Records

Phyoe Swe AUNG, Hiroshi KAWASE, Shinichi MATSUSHIMA, Fumiaki NAGASHIMA, Tun NAING(1) and Myo THANT(2)

(1) Professor and Head, Department of Engineering Geology, Yangon Technological University, Myanmar
(2) Professor, Department of Geology, Monywa University, Myanmar

Synopsis

For quantitative prediction of strong ground motions, we desperately need precise information of shear wave (S-wave) velocities down to the seismological bedrock for site effect estimation. To determine the deep S-wave velocity profiles in Sagaing City of Myanmar, we have used both single-station and array methods for microtremor records. In this study, we have conducted five microtremor array sites and 100 sites for single-station measurement. In order to estimate the S-wave velocity profile down to the seismic bedrock (Vs = 3.0 km/s), we extended the radii of the arrays sequentially and we obtained the Rayleigh wave phase velocity in the long-period range. After that, one dimensional S-wave velocity structure models for five array sites were determined. Then, S-wave velocity inversion for all single-station sites were carried out by referencing the five array models. According to the inversion results, we estimated that the engineering bedrock (Vs > 500 m/s) for Sagaing City exists in the range of 10 m to 80 m in depth.

Keywords: Array measurement, Phase Velocity, Shear Wave Velocity, MHVR, pEHVR, EMR

1. Introduction

The research area of this study, the Sagaing City, Myanmar is situated in central part of Myanmar and quite important because of its well-conducted cultural heritage. It is also a historically crucial city for Myanmar. Unfavorably, the most active and longest fault in Myanmar, namely Sagaing Fault, which is a right-lateral strike-slip fault and having a length of 1200 km (Swe, 1981), is running closely and has generated many destructive earthquakes with Magnitude 7 or more in 1839 and 1956.These earthquakes caused severe damage to several pagodas, several masonry buildings and killed some tens of people in the Sagaing area. In addition, studies have been conducted recently by Pailoplee (2013), and Hurukawa and Maung (2011), and they considered that there is a high probability of a large earthquake (up to Magnitude 7.9) occurring along the Sagaing Fault, and resulting large shaking especially in the Naypyidaw - Mandalay region, which is close to Sagaing City.

According to these facts, it is obvious that Sagaing City is a seismically prone city. Even though seismic hazards caused by the Sagaing Fault have been expected high in Sagaing City from the past till present, the detail seismic assessment is not conducted yet. It is a major issue for acquiring information about shear wave velocity structure (here in after S-wave velocity structure) for theoretical simulation of strong motions including the actual basin response. Due to this reason, current

research was conducted with the purpose of estimating the deep S-wave velocity profiles through microtremor measurements, which can be used for strong motion simulation and other seismic purposes.

Among the many geophysical exploration methods, it has been recognized that microtremor array technique is the most economic and easy-to-use tool because of its simple deployment compared to other noninvasive, conventional methods such as reflection and refraction surveys to explore the deep sedimentary layers.

Although there are numerous ways to evaluate the S-wave profiles from Rayleigh wave phase velocity of microtremor array, the well-established method that can determine the S-wave velocity structure down to the seismological bedrock (Vs = 3.0 km or higher) are not abundant. Over three decades ago, the exploration method to determine the deep basin structure using array records of long-period (>1sec) microtremor was successfully established by Horike (1985) and Matsushima and Okada (1990) after the pioneering work done by Aki (1957). Based on the success of these studies, the method has been extended to estimate both deep and shallow structures by others (e.g. Kawase et al., 1998).

Recently, Cho et al. (2004, 2006) presented the innovative method which is basically derived from the traditional theory of SPAC (Spatial Autocorrelation) Method by Aki (1957). Their method uses the vertical-motion records of microtremors, obtained at different locations around a single circle (no center station needed) to evaluate the phase velocities of Rayleigh waves. Later, Tada et al. (2007) offered the wealth of alternative methods to explore the phase velocities of Rayleigh waves by revising Cho et al. (2004, 2006). In the latest version of Tada et al. (2007) method, the Rayleigh wave phase velocities can be extracted by the methods called as CCA (Centerless Circular Array), and nc-CCA (noise-compensated CCA) in addition to Henstridge's (1979) methods. As this newly developed method by Tada et al. (2007) can provide the good resolution of different wavelength ranges of phase velocities, we applied their method in our study to estimate the S-wave velocity in case of one dimensional structure identification for Sagaing City.

2. Sites and Data Assessment

In order to estimate the deep S-wave velocity profile in Sagaing City, we conducted microtremor acceleration array measurement at five sites (hereafter we called them as ARRAY1, ARRAY2, ARRAY3, ARRAY4 and ARRAY5). Furthermore, we performed two additional microtremor velocity arrays (VSEAR1, and VSEAR2) by co-installing the velocity seismometers (hereafter VSE), in addition to the four accelerometers. The purpose is to expand the detection limit in the longer-period range and connect the phase velocities from former five array sites.

Since five sites of array were not sufficient to construct the three dimensional basin structure, we also performed the single-station measurement at 100 sites, covering the whole area of the city. The locations of the single station sites, microtremor array sites, and also two VSE array sites are plotted in Figure 1.

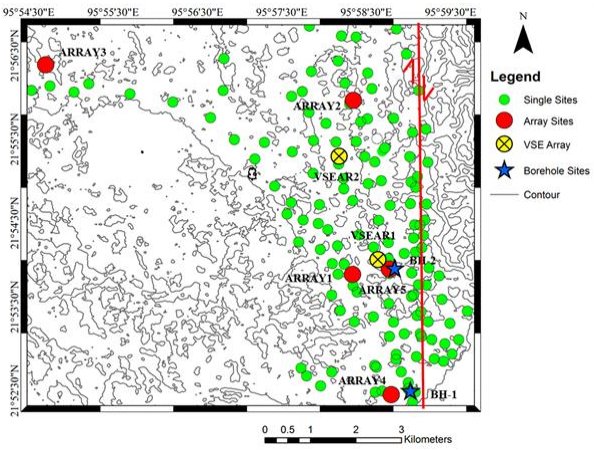

Fig. 1 Locations of microtremor observation sites in Sagaing City

As for the measurement for both single-station and array measurements of microtremors, three-component accelerometer SMAR-6A3P (Mitutoyo) combined with LS8800 data logger (Hakusan Corporation) as shown in Photo 1, was used. Particularly for the largest radius array (VSE array), we co-installed the tri-axial servo type velocity speedometer VSE-11 and VSE-12 (Tokyo Sokushin), as shown in Photo 2. As for the configuration of the array system, we performed the "four-point array" by arranging one seismometer at the center of a

circle and other three seismometers on the circumference, to form a triangular shape as displayed in Figure 2. We conducted the microtremor acceleration array measurement by using different radius for S, M, and L array as 30m, 50m, and 100m, respectively. However, for the two VSE array sites, we enlarged the array size for X, XL and XXL arrays to 300m, 600m and 1200m, respectively, and also increased the duration of the recording time, depending on the size of the array. The detailed explanation for array sizes, duration and observation systems are shown in Table 1. Then, we combined the VSE array data with acceleration array data based on their geographical location for the purpose of reaching to the longer wavelength.

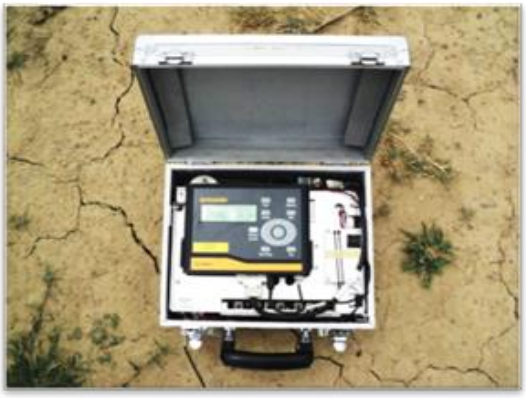

Photo 1 Instrument of SMAR with LS8800 Data Logger

For S and M arrays, we measured the relative coordinates of stations by measuring tapes. However, for L, X, XL and XXL arrays, we calculated the distances from latitudes and longitudes observed by a differential GPS (Global Positioning System). The accuracy of the internal clock was within 1 ppm and was corrected by the (GPS) before each measurement such that the instruments could make simultaneous observations. The timing accuracy from GPS correction was within 1 msec. The sampling frequency was 200 Hz and the amplifier was set to 500 times, and low-pass filter was fixed at 50 Hz. As for the single-station measurement, we performed it at 100 sites and recorded about 15 minutes per each site by using the grid spacing of approximately 0.5 km and sampling frequency was the same with array measurement (i.e. 200 Hz).

Photo 2 Instrument of tri-axial servo type velocity speedometer (VSE)

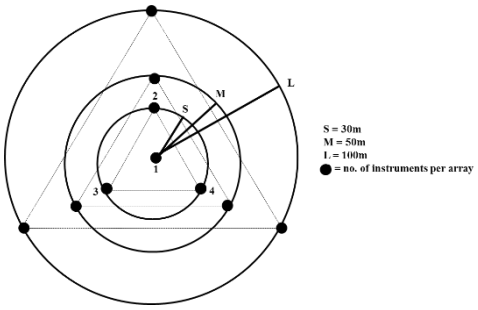

Fig. 2 Configuration of array measurement for S, M, and L array

Table 1 Detail information for observation system of arrays

Types of Array	Name of Array	Latitude	Longitude	Number of Stations	Sizes of array	Duration
Microtremor Acceleration Array	ARRAY1	21.8981	95.97227	4(one center+3 circumference of a circle)	S,M,L (30m, 50m, 100m)	30 minutes for each array size
	ARRAY2	21.9327	95.97245			
	ARRAY3	21.9398	95.91165			
	ARRAY4	21.8741	95.97993			
	ARRAY5	21.8991	95.97957			
Microtremor Velocity Array	VSEAR1	21.9010	95.97731	4(one center+3 circumference of a circle)	X (300m)	1 hour
					XL (600m)	30 min
					XXL (1200m)	40 min
	VSEAR2	21.9216	95.96964	4(one center+3 circumference of a circle)	X (300m)	30 min
					XL (600m)	30 min

3. Data Processing, Methodology and Results

3.1. Analysis to obtain Phase Velocities

Primarily two approaches have been used to obtain the phase velocity of the fundamental mode of Rayleigh waves from array measurement of microtremors at the target sites. The first one was proposed by Aki (1957) by utilizing small-scale circular seismic arrays, which can provide the phase velocity dispersion curve by correlating noise

records using a SPAC method. On the other hand, Capon (1969) introduced a high-resolution method using the maximum-likelihood of frequency-wave number (so called f-k method) to determine the vector velocity of propagating seismic waves of large aperture seismic arrays.

In this study, we adopted the BIDO program (version 2.0) by Tada et al. (2007) to identify the Rayleigh wave phase velocities of the sedimentary layers., Basically their method is the natural extension from the assumption of the SPAC method as stated above. If we say more precisely, we estimated the phase velocities by nc-CCA method.

The nc-CCA method is based on the algorithm of the CCA method, which identifies the phase velocities by compensating for the effects of incoherent noise. The nc-CCA method is intended for eliminating the analysis limit for the long wavelength side of the CCA method and we obtained the phase velocity (c) using the following Equation 1, which is deduced by adopting the long-wavelength approximation of the Bessel function in Equation 2, under the assumption that the wavelength is sufficiently longer than the array radius r,

$$c = \pi f r \sqrt{\frac{2+\rho_{cca}}{1+\frac{\varepsilon}{N}+\frac{\delta\rho_{cca}}{N}}} \quad (1)$$

$$\rho_{cca} = \frac{J^2 0(rk)}{J^2 1(rk)} = g(rk, 0, N) \quad (2)$$

Where f is the frequency, k is the wavenumber and N is the number of seismometers. The Noise-to-Signal (SN) ratio ε can be identified by using the following Equation 3,

$$\varepsilon = \frac{-B \pm \sqrt{B^2 - 4AC}}{2A} \quad (3)$$

$$A = -\rho^2,$$

$$B = \frac{\rho^2}{coh^2} - 2\rho^2 - \frac{1}{N}$$

$$C = \rho^2\left(\frac{1}{coh^2} - 1\right)$$

The variable ρ is the SPAC coefficient originally defined in Aki (1957), which can be achieved by directionally averaging the cross-spectral densities between the records on the circumference and at the center point, and then normalizing by the power spectral density at the center point. The variable coh^2 is the magnitude-squared coherence. The resulted dispersion curves of the phase velocity for five array sites through the nc-CCA method are presented in Figure 3.

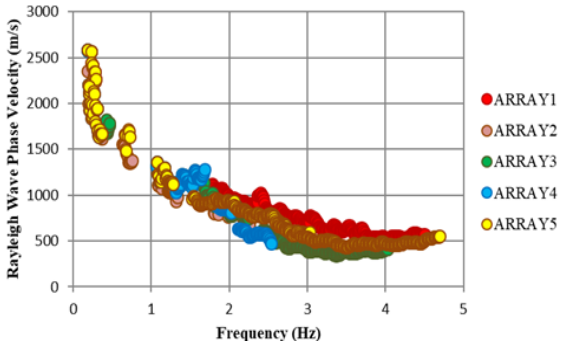

Fig. 3 Results of phase velocity dispersion curves for 5 array sites by nc-CCA method

3.2 Inversion of S-wave Velocity Structure

In order to prepare the initial model, we converted the dispersion curve to the S-wave velocity profiles by using the traditional method by Ballard (1964), from the following relations,

$$Z = \frac{1}{3}\lambda, \quad Vsz = 1.1\, C\lambda \quad (4)$$

where, Z refers to the depth (m), Vsz means S-wave velocity at depth Z (m/sec) and Cλ means phase velocity (m/sec) at λ, wavelength. In Figure 4, we offered the results of the inverted S-wave velocity profiles for five array sites. The identified initial array model for ARRAY1 site using with Ballard method is stated in Figure 5.

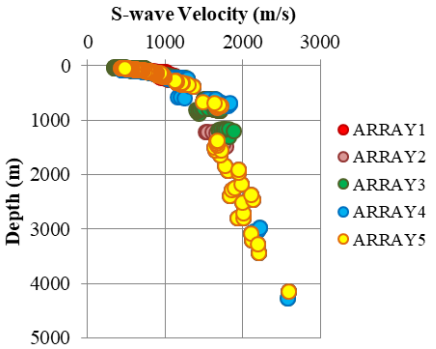

Fig. 4 Inverted S-wave velocity profiles for 5 array sites

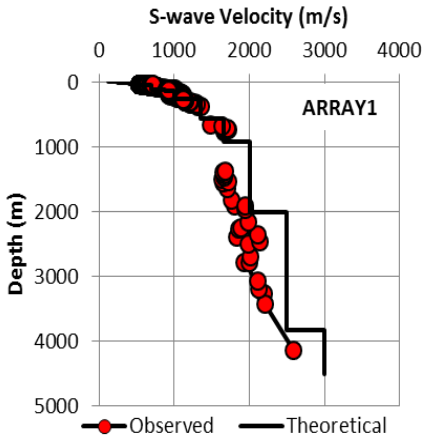

Fig. 5 Identified initial structure model for ARRAY 1 site with Ballard method

Once we obtained the initial models using Ballard (1964) method, we identified the final structure models by two alternative methods of García-Jerez et al. (2016) and Nagashima et al. (2014). Primarily, method of García-Jerez et al. (2016) is based on the assumption of diffuse field theory by Sánchez-Sesma et al. (2011) and it can provide the S-wave velocity structure model with the simultaneous inversion of dispersion curve (here in after DC) and horizontal-to-vertical spectral ratio (here in after H/V) based on microtremor horizontal-to-vertical spectral ratios (MHVRs). In contrast, Nagashima et al. (2014) inverts the velocity structure using earthquake horizontal-to-vertical spectral ratios (EHVRs). Due to this reason, our purpose is to identify the similar S-wave velocity structure models from these two different approaches.

As for the process of development of our models, first, we identified the five array models for five different sites using the method by García-Jerez et al. (2016). Since we already idealized the initial model using Ballard (1964) method before this stage, we could save time and effort to perform trial inversions in current step and also would expect to get better velocity structure models. After that, we averaged those five array models resulted from the method of García-Jerez et al. (2016) in order to get the average model in the area. Then, we used this average model as an initial model to perform the inversion technique by Nagashima et al. (2014).

As stated above, our purpose is to search for the similar structure model between the two methods, and therefore, we limited the searching range of parameters from the initial average model; i.e. we searched for the thickness of each layer within the range of ± 30% from the initial model, while S-wave velocity (Vs) values were fixed. Although we identified the similar structure models based on different approaches, we achieved to get equivalent structure models which give quite good matching to H/V spectral ratios as showed in Figure 6. The detail of the resulted final velocity structure models for five array sites including their material properties were stated in Table 2.

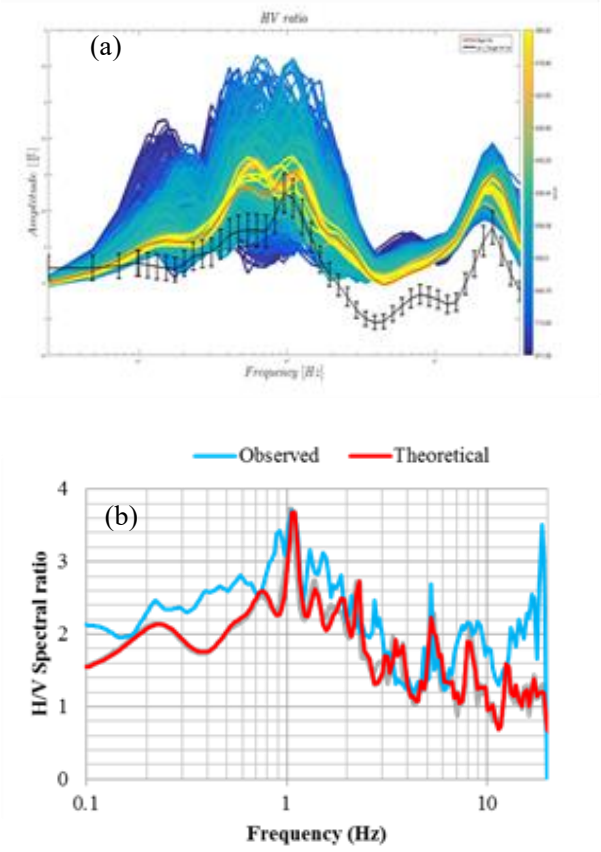

Fig. 6 Comparison of agreement of H/VRs between theoretical and observation (a) García-Jerez et al. (2016) method and (b) Nagashima et al. (2014)

3.3 S-wave Velocity Inversion for Single Station Sites

To perform the S-wave velocity inversion for all single station sites, first we divided the all single station sites as five zones based on the geographically proximity to the five array sites. After that, we performed the inversion for all single station sites by referencing the five array models from previous section as an initial models using with

Nagashima et al. (2014) method together with earthquake-microtremor ratio (EMR) function proposed by Kawase et al. (2018) and here are some descriptions for utilization of their methods.

Table 2 Results of estimated final velocity structure models for 5 array sites

ARRAY1

Layers	Thickness (m)	Depth (m)	Vs (m/s)	Vp (m/s)	Gam (g/cm³)
1	1.5	1.5	149	935	1.66
2	1.5	3	247	1139	1.73
3	10	13	332	1312	1.79
4	23	36	404	1457	1.83
5	21	57	489	1625	1.87
6	52	109	651	1939	1.94
7	48	157	893	2388	2.03
8	67	224	992	2566	2.07
9	256	480	1374	3216	2.19
10	332	812	1568	3526	2.24
11	978	1790	1987	4145	2.34
12	1105	2895	2528	4846	2.47
13	∞	∞	3000	5368	2.56

ARRAY2

Layers	Thickness (m)	Depth (m)	Vs (m/s)	Vp (m/s)	Gam (g/cm³)
1	1.5	1.5	149	935	1.66
2	1.5	3	247	1139	1.73
3	7	10	332	1312	1.79
4	13	23	404	1457	1.83
5	15	38	489	1625	1.87
6	30	68	651	1939	1.94
7	48	116	893	2388	2.03
8	67	183	992	2566	2.07
9	291	474	1374	3216	2.19
10	311	785	1568	3526	2.24
11	978	1763	1987	4145	2.34
12	1105	2868	2528	4846	2.47
13	∞	∞	3000	5368	2.56

ARRAY3

Layers	Thickness (m)	Depth (m)	Vs (m/s)	Vp (m/s)	Gam (g/cm³)
1	1.5	1.5	149	935	1.66
2	1.5	3	247	1139	1.73
3	7	10	332	1312	1.79
4	13	23	404	1457	1.83
5	15	38	489	1625	1.87
6	30	68	651	1939	1.94
7	88	156	893	2388	2.03
8	124	280	992	2566	2.07
9	284	564	1374	3216	2.19
10	491	1055	1568	3526	2.24
11	978	2033	1987	4145	2.34
12	1105	3138	2528	4846	2.47
13	∞	∞	3000	5368	2.56

ARRAY4

Layers	Thickness (m)	Depth (m)	Vs (m/s)	Vp (m/s)	Gam (g/cm³)
1	1.5	1.5	149	935	1.66
2	1.5	3	247	1139	1.73
3	8	11	332	1312	1.79
4	13	24	404	1457	1.83
5	15	39	489	1625	1.87
6	30	69	651	1939	1.94
7	68	137	893	2388	2.03
8	67	204	992	2566	2.07
9	303	507	1374	3216	2.19
10	492	999	1568	3526	2.24
11	978	1977	1987	4145	2.34
12	1105	3082	2528	4846	2.47
13	∞	∞	3000	5368	2.56

ARRAY5

Layers	Thickness (m)	Depth (m)	Vs (m/s)	Vp (m/s)	Gam (g/cm³)
1	1.5	1.5	149	935	1.66
2	1.5	3	247	1139	1.73
3	7	10	332	1312	1.79
4	13	23	404	1457	1.83
5	29	52	489	1625	1.87
6	48	100	651	1939	1.94
7	61	161	893	2388	2.03
8	67	228	992	2566	2.07
9	305	533	1374	3216	2.19
10	368	901	1568	3526	2.24
11	978	1879	1987	4145	2.34
12	1105	2984	2528	4846	2.47
13	∞	∞	3000	5368	2.56

3.3.1 Nagashima et al. (2014) method and EMR Function

The S-wave velocity inversion scheme for all single station sites applied in this study was the one proposed by Nagashima et al. (2014) and their inversion scheme was based on the Hybrid Heuristic Search (HHS) method by Yamanaka et al. (2007).

According to Kawase et al. (2018), they compared the EHVRs and MHVRs, and the results showed more or less similar until the first peak frequency. However, they are significantly different in higher frequency range and this is because MHVRs mainly consists of surface waves so that peaks associated with higher modes would not be so prominent as those of EHVRs. Due to this reason, they developed an empirical translation procedure from MHVRs to EHVRs by using the EMR function. The resultant EHVRs are called pseudo EHVRs (or pEHVRs). They also found that using pEHVR we can identify the velocity structures with much better correspondence to the true structure rather than the direct application of MHVRs to the inversion. Due to these facts, we transformed the MHVRs into pEHVR before performing the inversion step by Nagashima et al. (2014).

EMR function was developed by Kawase et al. (2018), which can convert MHVRs into pEHVR as stated below. Basically, EMR is classified, based on their clear first peak frequencies, into five different categories (0.2 to 1 Hz, 1 to 2 Hz, 2 to 5 Hz, 5 to 10 Hz and 10 to 20 Hz). Then, pEHVR is identified by multiplying MHVRs with EMR from the following Equation 5,

$$\text{Pseudo EHVR} = \text{MVHRs} * \text{EMR} \quad (5)$$

where, EMR is the ratio of the average EHVR with respect to the MHVRs as shown in this relation by Equation 6;

$$\text{EMR} = \text{EHVR} / \text{MHVR} \quad (6)$$

3.3.2 Inversion Results

As for the inversion analysis for all single station sites, we applied the Nagashima et al. (2014) method after assuredly transforming MHVRs to pEHVR via EMR function, as described in above section. Since we assumed that the impendent contrast of S-wave velocity is strongly influenced in shallow part (Vs < 500 m/s) for Sagaing City, we changed only ± 50 % from the initial model for both Vs and thickness values in shallow layers, while deep layers are fixed. In order to optimize the residual or misfit values as stated in Equation 7, we performed inversion for 10 times for each site.

$$\text{Misfit} = \Sigma \log (\text{EHVR}_{obs}) - \log (\text{EHVR}_{the})^2/f \quad (7)$$

Where f = frequency, is calculated and after the trial of inversion for 10 times, we chose the best model among the 10 trials. In each inversion, we used 200 generations, 400 populations and set at the cross rate as 0.7 and mutation rate as 0.1. The damping ratio was assumed as 0.01 for all cases. In Figure 7, we illustrated the comparison between MHVR and pEHVR for ten selected sites and their ten times inversion and resulted velocity structures are

presented in Figure 8. As we can see the reproduction of the pEHVR by the inverted structure is good for the frequency range from 0.6 Hz to 20 Hz. The resultant velocity structures are different mostly in the shallow part, where the depths to the engineering bedrock, i.e., the layer with the S-wave velocity higher than 500m/s, is varying from 10 m to 80 m from site to site, The site amplification characteristics would be different accordingly so that we should reflect these differences in our strong motion prediction.

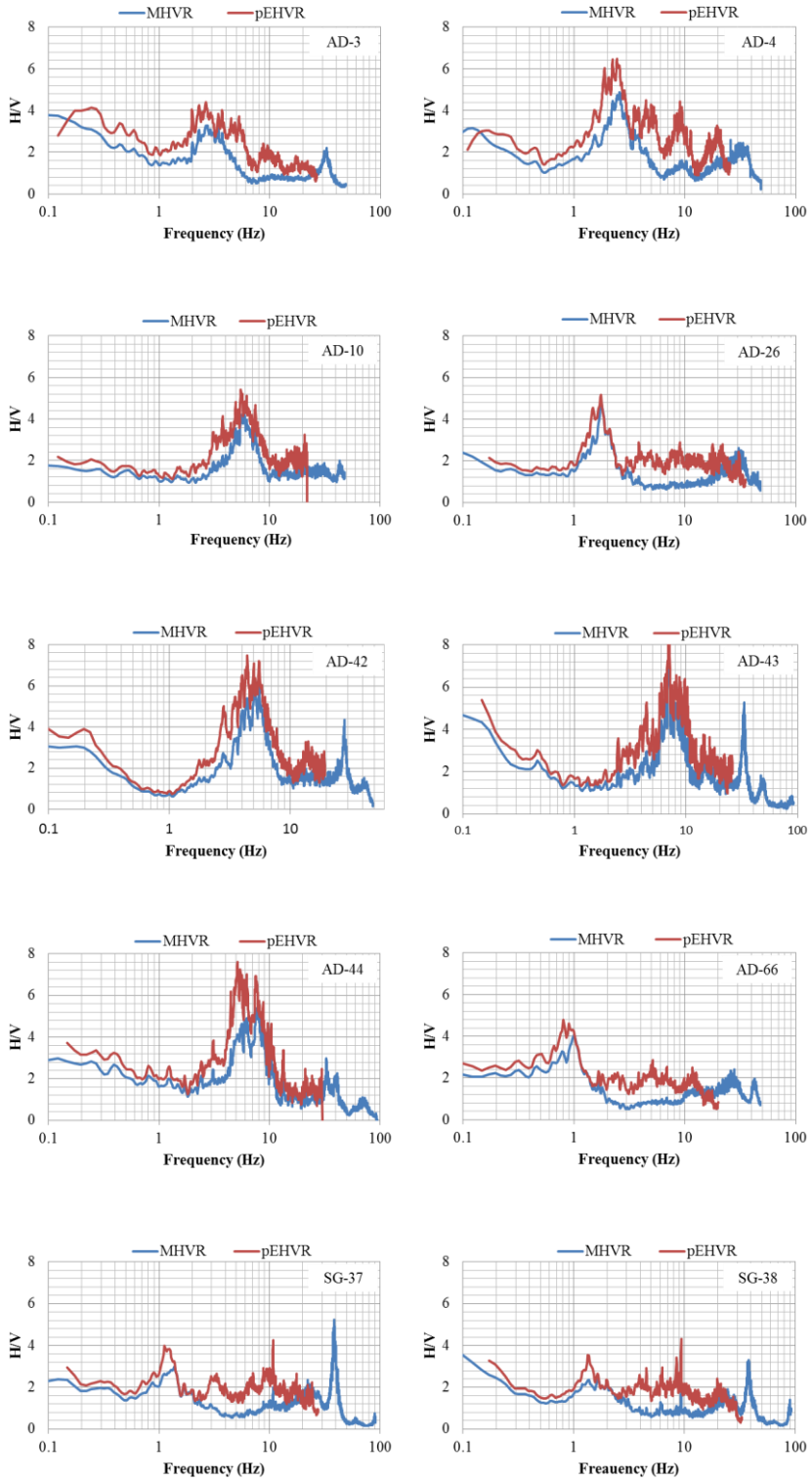

Fig. 7 Comparison of MHVR (blue line) and pEHVR (red line) for ten selected sites

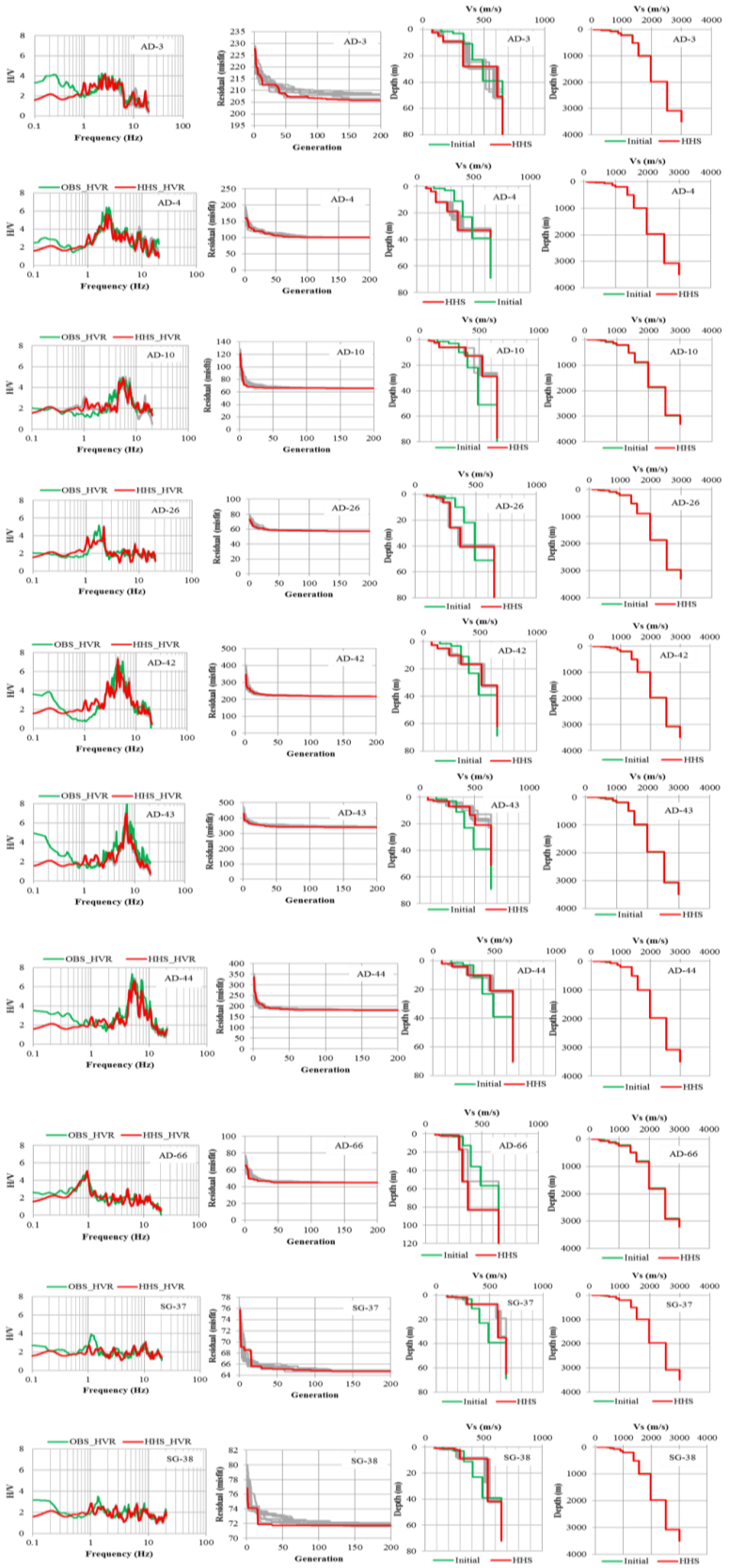

Fig. 8 The best-fit model from HHS inversion of shallow and deep of S-wave velocities at ten selected sites. In every figures, green lines refer to observed HVRs (pEHVR) or the velocity structures of the initial models and the red lines represent the best model among the ten time trials from productive HVRs of HHS method. The grey lines are those ten time trials with different genes.

4. Conclusions

In this study, we conducted analysis using microtremor data in order to estimate the deep S-wave velocity profiles for Sagaing City, since the information of subsurface velocity structure is necessary for estimating the seismic response for this city. In order to achieve this, we measured five microtremor array sites together with 100 single station measurements to cover the whole area of the city. For the analysis of array measurements, we used nc-CCA method and attained stable phase velocities for each array site. After that, we converted those phase velocity information as 1D S-wave velocity profiles by means of inversion techniques. As the accomplishment, we identified the 13 layers models for five array sites which are reaching to the seismic bedrock of Vs having 3.0 km/s. Subsequently, S-wave velocity structures for all single station sites were estimated by referring to those five array models. Our forthcoming study is to create the 3D basin structure model through this study and to perform the strong motion simulation along the Sagaing Fault in order to support the appropriate seismic microzonation hazard maps for Sagaing City, Myanmar.

Acknowledgements

The authors would like to express our gratitude to authorized persons from Sagaing City for their various assists in the microtremor observations. Students from DPRI, Kyoto University and Yangon University are acknowledged for their collaboration during the field trip in Myanmar. The first author is supported by JICA (AUNSEED/Net) program for her PhD study.

References

Aki, K. (1975): Space and time spectra of stationary stochastic waves, with special reference to microtremors, Bull. Earthquake Res. Inst., Tokyo Univ, Vol. 35, pp. 415-456.

Ballard R.F. (1964): Determination of ground shears moduli at depth by in situ vibratory techniques, U.S. Army Engineer Waterways Experiment Station, Vicksburg, Miss., No. 4, pp. 691.

Capon J. (1969): High resolution frequency wavenumber spectrum analysis, Pro. IEEE, Vol. 57, pp. 1408-1418.

Cho I., Tada T., and Shinozaki Y. (2004): A new method to determine phase velocities of Rayleigh waves from microseisms, Geophysics, Vol. 69 (6), pp. 1535-1551, 10.1190/1.1836827.

Cho I., Tada T., and Shinozaki Y. (2006): Centerless circular array method: Inferring phase velocities of Rayliegh Waves in broad wavaelength ranges using microtremor records, J. Geophys. Res, AGU, 111:B09315, doi: 10.1029/2005JB004235.

García-Jerez A., Piña-Flores J., Sánchez-Sesma F.J., Luzón F., Perton M. (2016): A computer code for forward calculation and inversion of the H/V spectral under the diffuse field assumption, Computers & Geosciences, Vol. 87, pp. 67-78. doi: 10.1016/j.cageo.2016.06.016.

Henstridge, J.D. (1979): A signal processing method for circular arrays, Geophysics, Vol. 44, pp. 179-184.

Horike M. (1985): Inversion of phase velocity of long-period microtremors to the S-wave velocity structure down to the basement in urbanized areas, J. Phys. Earth, Vol.33, pp. 59-96.

Hurukawa N. and Maung P.M. (2011): Two seismic gaps on the Sagaing Fault, Myanmar, derived from relocation historical earthquakes since 1918, Geophys. Res. Lett., Vol. 38, Lo1310, doi: 10.1029/2010GL046099.

Kawase H., Satoh T., Iwata T., Irikura K. (1998): S-wave velocity structures in the San Fernando and Santa Monica area, Proceedings of the 2nd International Symposium on Effects of Surface Geology on Seismic Motions, Tokyo, Japan, Vol. 2, pp. 733-740.

Kawase H., Mori Y., Nagashima F. (2018): Difference of horizontal-to-vertical spectral ratios of observed earthquakes and microtremors and its application to S-wave velocity inversion based on the diffuse field concept, Earth, Planets and Space, Vol. 70:1, doi:10.1186/s40623-017-0766-4.

Matsushima T., Okada H. (1990): Determination of deep geological structures under urban areas using long-period microtremors, Butsuri Tansa, Vol. 43, pp. 21-33.

Nagashima F., Matsushima S., Kawase H., Sánchez-Sesma F.J., Hayakawa T., Satoh T., Oshima M.

(2014): Application of horizontal-to-vertical (H/V) spectral ratios of earthquake ground motions to identify subsurface structures at and around the K-NET site in Tohoku, Japan, Bull. Seismol. Soc. Ami.,104:22882302.https://doi.org/10.1785/01201 30219.

Pailoplee S. (2013). Mapping asperities along the Sagaing Fault zone, Myanmar using b-values anomalies, Journal of Earthquake and Tsunami, Vol. 7,No.5,1371001,doi:10.1142/ SI793431113710012.

Swe W. (1981): A major strike-slip fault in Burma, Contrib. Burmese Geol., Vol. 1(1), pp. 63-67.

Satoh T., Kawase H., Iwata T., Higashi S., Sato T., Irikura K., Huang H.C (2001): S-wave velocity structure of the Taichung basin, Taiwan, estimated from array and single-statin records of microtremors, Bull. Seismol. Soc. Ami., Vol. 91 (5), pp. 1255-1266.

Sánchez-Sesma F. J., Rodríguez M., Iturrarán-Viveros U., Luzón F., Campillo M., Margerin L., García-Jerez A., Suarez M., Santoyo M. A., and Rodríguez-Castellanos A., (2011): A theory for microtremor H/V spectral ratio: application for a layered medium, *Geophysical Journal International Express Letters* **186** (1) 221-225, doi: 10.1111/j.1365-246X.2011.05064.x.

Tada T., Cho I., and Shinozaki Y. (2007): Beyond the SPAC method: Exploiting the wealth of circular-array methods for microtremor exploration, Bull. Seimol. Soc. Ami., Vol. 97(6), 2080-2095.

Yamanaka H. (2007): Inversion of surface wave phase velocity using hybrid heuristic search method, BUTSURI-TANSA, 60:265-257 (in Japanese with English abstract).

(Received June 12, 2018)